ACS chemical biology

Articles

pubs.acs.org/acschemicalbiology

Visualization and Quantitative Analysis of G Protein-Coupled Receptor–β-Arrestin Interaction in Single Cells and Specific Organs of Living Mice Using Split Luciferase Complementation

Hideo Takakura, Mitsuru Hattori, Masaki Takeuchi, and Takeaki Ozawa*

Department of Chemistry, School of Science, The University of Tokyo, 7-3-1 Hongo, Bunkyo-ku, Tokyo 113-0033, Japan

Supporting Information

ABSTRACT: Methods used to assess the efficacy of potentially therapeutic reagents for G protein-coupled receptors (GPCRs) have been developed. Previously, we demonstrated sensitive detection of the interaction of GPCRs and β-arrestin2 (ARRB2) using 96-well microtiter plates and a bioluminescence microscope based on split click beetle luciferase complementation. Herein, using firefly luciferase emitting longer wavelength light, we demonstrate quantitative analysis of the interaction of β2-adrenergic receptor (ADRB2), a kind of GPCR, and ARRB2 in a 96-well plate assay with single-cell imaging. Additionally, we showed bioluminescence *in vivo* imaging of the ADRB2–ARRB2 interaction in two systems: cell implantation and hydrodynamic tail vein (HTV) methods. Specifically, in the HTV method, the luminescence signal from the liver upon stimulation of an agonist for ADRB2 was obtained in the intact systems of mice. The results demonstrate that this method enables noninvasive screening of the efficacy of chemicals at the specific organ in *in vivo* testing. This *in vivo* system can contribute to effective evaluation in pharmacokinetics and pharmacodynamics and expedite the development of new drugs for GPCRs.

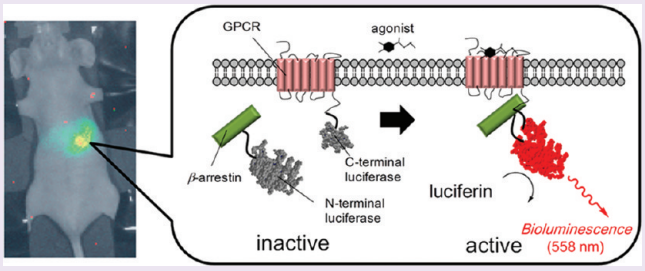

Molecules of the largest class of integral membrane receptors, G protein-coupled receptors (GPCRs), respond to an enormous array of stimuli including growth factors, hormones, and neurotransmitters. These molecules regulate many physiological functions[1] and are involved in some disease conditions, such as diabetes, cancer, obesity, inflammation, and pain, making them a top target class for pharmaceuticals.[2−5] Therefore, several approaches to discovery of the new therapeutic reagents for GPCRs have been conducted.[5,6] Classically, binding assays using radioactive ligands have been used to identify compounds that bind to GPCRs.[7,8] However, this method has several major shortcomings: (i) it necessitates complicated protocols and careful manipulation for radioactive compounds, (ii) it relies absolutely on radiolabeled ligands, and (iii) it cannot readily distinguish between the functional properties of ligands. Accordingly, current main approaches have moved to cell-based functional assays. Generally, the assays for GPCRs are based on receptor activation and intracellular signaling, such as Ca^{2+} or adenosine 3′,5′-cyclic monophosphate (cAMP). The detection of such signals requires indicators for Ca^{2+} [9−11] and genetically encoded probes for cAMP.[12−14] These methods can easily measure the signal for production of second messengers and are suitable for high-throughput screening (HTS) using 96-, 384-, or 1536-well plates. However, a major issue is detection of many false positive compounds that activate the downstream pathway inside cells through other signaling cascades.

Other methods that overcome this problem include the use the phenomenon of β-arrestin translocation to GPCR. Upon activation of GPCRs by some ligands, cytosolic β-arrestin proteins translocate to the plasma membrane and interact with the activated and phosphorylated receptors. This recruitment is applicable to a functional readout for therapeutic compounds of GPCRs, for example, bioluminescence resonance energy transfer (BRET) technology using *Renilla* luciferase and fluorescent proteins,[15−17] and reporter gene assays in which the release of transcriptional factor is triggered by β-arrestin recruitment through the intermediary of cleavage of specific protease.[18,19] These methods showed good signal-to-noise ratios and are also amenable to HTS. Nevertheless, so far, the application has remained limited use in *in vitro* assays. To investigate properties of drug candidates closely, it is important to develop a method for use in highly biological systems, including single living cells and animal models, even in deeper tissues such as organs. Recently, we and other groups have reported novel methods based on a complementary technology for such systems.[20−23] The principle is that reporter proteins, which are enzymes such as luciferase and β-galactosidase (β-gal), are divided into two fragments so that they lose the enzymatic activity. When the fragments of reporter proteins are brought within proximity, they spontaneously refold and

Received: September 12, 2011
Accepted: February 24, 2012
Published: February 24, 2012

   dx.doi.org/10.1021/cb200360z | ACS Chem. Biol. 2012, 7, 901–910

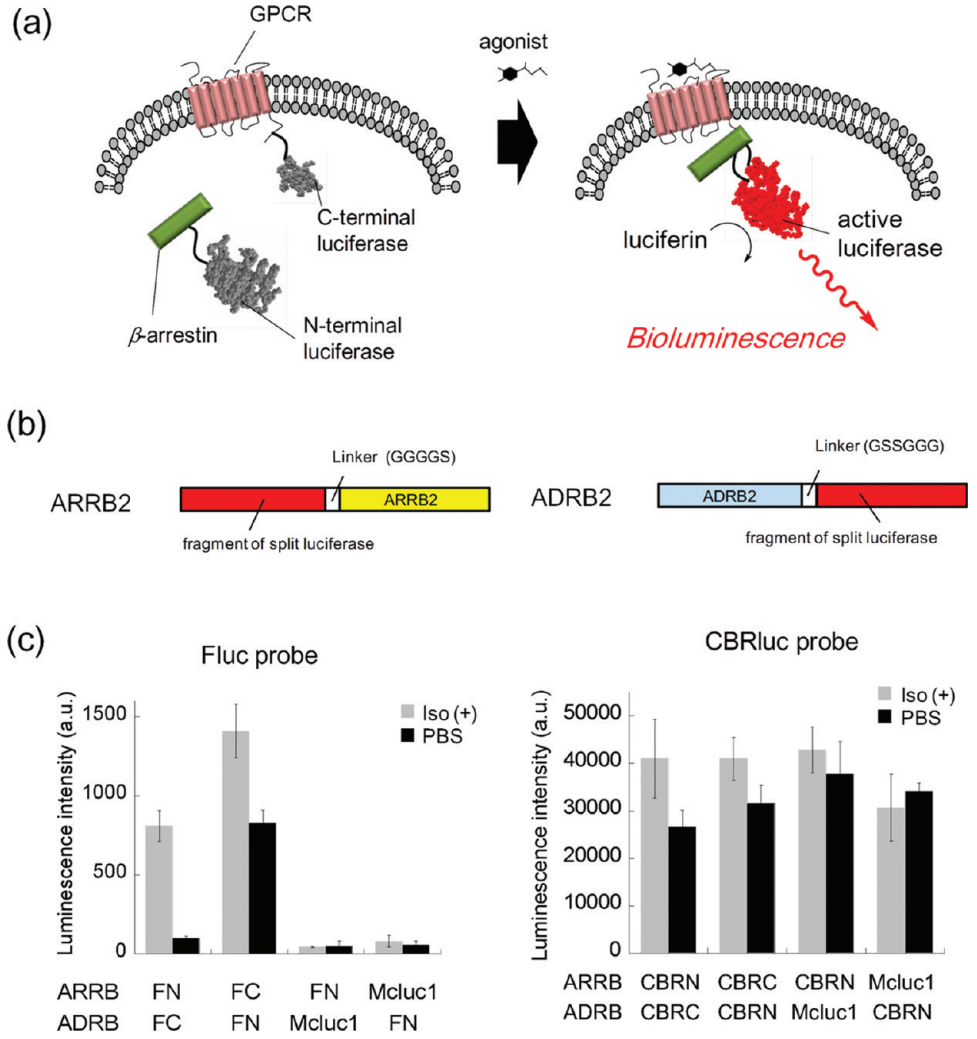

Figure 1. (a) Schematic diagram of the complementation strategy showing fusion of the N-terminal and C-terminal luciferase fragments to the GPCR and the cytoplasmic β-arrestin protein, respectively. An agonist binding to GPCR recruits β-arrestin to intracellular domains in the receptor, bringing each luciferase fragment into proximity and reconstituting luciferase activity to emit bioluminescence in the presence of luciferin. (b) Schematic structures of cDNA constructs. Fragment of split luciferase contains FN and FC, the N-terminal and C-terminal fragments of Fluc (1−415 aa for N-terminal, 413−549 aa for C-terminal), CBRN and CBRC, the N-terminal and C-terminal fragments of CBRluc (1−413 aa for N-terminal, 395−542 aa for C-terminal), and Mcluc1, the multiple-complement luciferase fragment. (c) Bioluminescence upon stimulation with Iso using HEK293 cells transiently coexpressing ARRB2 and ADRB2 fused to split luciferase fragments. The transfected cells were cultured on 96-well microtiter plates and stimulated with 1×10^{-5} M isoproterenol (Iso) for 15 min at 37 °C. The luminescence intensity was measured (n = 4).

reconstitute their function. Therefore, the restored enzymatic activity can be detected as an indicator of protein−protein interactions. We demonstrated that split click beetle luciferase is applicable to *in vitro* plate assays and single-cell imaging using a bioluminescence microscope.[23] In this method, green-emitting luciferase was used, which is unsuitable for *in vivo* imaging because of bad tissue penetration. In addition, other groups showed the GPCRs−β-arrestin interaction is detectable in *in vitro* assays and even *in vivo* using bioluminescence.[20,22] However, for *in vivo* imaging, the detection region was limited to the skin surface. GPCRs are expressed in many organs, and therefore ultimately the function in different organs is important for drug evaluation.

Herein, we demonstrate a universal monitoring method of GPCR−β-arrestin interaction in *in vitro* plate assays, single-cell imaging, and *in vivo* imaging using split firefly luciferase emitting yellow light. We show a technique to visualize GPCR−β-arrestin interaction from deep tissues such as a mouse liver. This *in vivo* system can contribute to the effective evaluation of reagents in pharmacokinetics and pharmcodynamics and accelerate the development of new drugs for GPCRs.

RESULTS AND DISCUSSION

Design of Split Luciferase Probes Emitting Longer-Wavelength Light. Previously, we developed a novel green-emitting split luciferase (Brazilian *Pyrearinus termitilluminans*; Eluc, λ_{max} = 537 nm) probe to detect the interaction between GPCRs and β-arrestin2 (ARRB2) (Figure 1a). After activation of GPCRs, the luminescence signal increased within 40 min and showed good signal-to-noise ratios in *in vitro* plate assays and single-cell imaging with bioluminescence microscopy.[23] However, for *in vivo* imaging, emission light with longer wavelength would be much better than green light from Eluc because yellow or red light offers good tissue penetration owing to minimal interference from hemoglobin.[24,25] Accordingly, yellow- and red-emitting firefly luciferase (North American *Photinus pyralis*; Fluc, λ_{max} = 558 nm) and click beetle in red

dx.doi.org/10.1021/cb200360z | ACS Chem. Biol. 2012, 7, 901−910

(Caribbean *Pyrophorus plagiophthalamus*; CBRluc, λ_{max} = 613 nm) have been used, respectively, for *in vivo* imaging of the interaction of GPCRs with β-arrestin. According to our earlier report,[26] the dissection site was determined. The N-terminal and C-terminal fragments of Fluc (FN and FC, respectively) consist of 1−415 and 413−549 amino acids of Fluc. The N-terminal and C-terminal fragments of CBRluc (CBRN and CBRC) consist of 1−413 and 395−542 amino acids of CBRluc. Among GPCRs of various kinds, we specifically examined the interaction of β2-adrenergic receptor (ADRB2) with ARRB2 because it is an important therapeutic target for sugar metabolism such as glycogenolysis and gluconeogenesis. The liver is a major site of expression. Monitoring of the function in the mouse liver is extremely important for pharmacokinetics and pharmacodynamics. Regarding design for construct of probes, the N-terminal end of ARRB2 or C-terminal end of ADRB2 was connected with the fragments of split luciferase probe, *e.g.*, FN, FC, CBRN, CBRC, and Mcluc1, which can be complemented with all N-terminals of split luciferase[26] (Figure 1b).

The activation of eight pairs of ARRB2 and ADRB2 fused to the split luciferase fragments upon stimulation by agonist for ADRB2, isoproterenol (Iso), was investigated with HEK293 cells to confirm the optimal pair. When we used the pair of FN-ARRB2 and ADRB2-FC, the best activation was obtained, which was 8-fold higher than that without stimulation (Figure 1c). Other pairs were less than 2-fold higher than addition of phosphate-buffered saline (PBS) because the efficiency of complementation with each fragment was decreased significantly by changes of the fragments from optimal positions. Also, we made two probes based on the red-shifted Fluc mutants (S284T and A348V) and compared the mutants with the wild type Fluc. The luminescence intensities obtained from the mutant probes upon stimulation with Iso were significantly lower about one-fourth for S284T and one-eighth for A348V compared to that of wild type (Supplementary Figure S3).

***In Vitro* Plate Assays Using a Stable Cell Line Carrying Split Luciferase Probes.** For *in vitro* plate assays, we established a stable cell line expressing FN-ARRB2 and ADRB2-FC. We obtained a specific clone named HEK293_FN-ARRB2_ADRB2-FC, whose intensity upon stimulation with Iso was increased to 43-fold higher than that under no stimulation (Figure 2a). The signal-to-noise ratios were 4-fold higher than that of our previous system.[23] The intracellular localization of FN-ARRB2 and ADRB2-FC in the presence and absence of Iso was confirmed using immunostaining. The results presented in Figure 2b showed that FN-ARRB2 was localized in the cytosol without Iso, whereas in the presence of Iso, FN-ARRB2 was located to the plasma membrane. The localization of ADRB2-FC was observed in the plasma membrane, although the dot-like structure was formed by addition of Iso attributable to internalization in cytosol. These results are evidence that complementation of split luciferase fragments was induced by translocation of ARRB2 from cytosol to the plasma membrane. In addition, we examined the bioluminescence spectra upon stimulation with Iso in *in vitro* assays and living cells and confirmed that the luminescence wavelength of split Fluc was almost identical to that of full-length Fluc (Supplementary Figure S2).

Using the HEK293_FN-ARRB2_ADRB2-FC cell line, we investigated the concentration dependency of various agonists such as Iso, metaproterenol (Meta), ritodrine (Rito), terbutaline (Ter), and dobutamine (Dobu) in *in vitro* 96-well plate

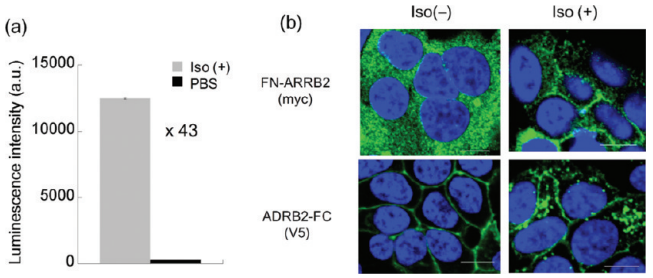

Figure 2. Establishment of HEK293 cells stably expressing split luciferase probe emitting longer wavelength. (a) Bioluminescence upon stimulation with Iso using HEK293_FN-ARRB2_ADRB2-FC cells. Measurements were performed for 2 s/well with a microplate reader (n = 4). (b) Immunocytochemical images of HEK293_FN-ARRB2_ADRB2-FC cells. The cells were incubated for 15 min in the presence and absence of 1 × 10^{-6} M Iso (final). The ADRB2 and ARRB2 were recognized by anti-V5 and anti-myc antibodies, respectively. The nuclei were stained with Hoechst 33342; superimposed images are shown. Scale bar: 10 μm.

assays. Bioluminescence was measured for 2 s/well using a plate reader. The raw data are shown in Figure 3a. Incubation with those agonists produced dose-dependent increases in bioluminescence with various activation ratios. The order was Iso > Ter > Meta ≫ Rito > Dobu; the luminescence intensity indicates the amount of ADRB2−β-arrestin interaction. Because ADRB2 binds to the G_s protein that activates adenylyl cyclase (AC), the production of cAMP depends on activity of ADRB2. Therefore, the amount of ADRB2−β-arrestin interaction might correlate with the production of cAMP. We compared the luminescence intensity with the results of the production of cAMP using agonists for ADRB2, which has been reported previously.[27−29] As a result, we found that the order of luminescence intensity obtained upon stimulation with each agonist was concomitant with the production of cAMP. In addition, EC_{50} values of these compounds varied, namely, Iso < Rito < Ter = Dobu < Meta. Next, we examined inhibition assays for Iso using competitive inhibitors for ADRB2 such as propranolol (Prop), pindolol (Pind), and butoxamine (Buto). To confirm the property of these compounds as a competitive inhibitor, dose−response curves of bioluminescence for Iso in the presence of a fixed concentration of each inhibitor were examined (Figure 3b). Pretreatment with different inhibitor for 30 min led to parallel shifts of the curve toward high concentrations of Iso, suggesting that these compounds functioned as typical competitive inhibitors. The IC_{50} values of these compounds against Iso were measured and calculated (Figure 3c). Several IC_{50} and EC_{50} values were consistent with those of a previous report.[30] These results underscored the applicability of HEK293_FN-ARRB2_ADRB2-FC for selective and quantitative assessment of the effect of ligands on ADRB2 in good signal-to-noise ratios.

Real-Time Imaging of the ADRB2−ARRB2 Interaction in Single Living Cells. To demonstrate the applicability of HEK293_FN-ARRB2_ADRB2-FC, we tried to visualize the ADRB2−ARRB2 interaction in real time under bioluminescence microscope. Upon stimulation with 1 μM Iso, a large increase in bioluminescence was observed only at the plasma membrane of the cells within 20 min (Figure 4a,b and Supplementary Movie S1). Successively, the localization of the bioluminescence changed gradually into the cytosol, suggesting that internalization of the ADRB2−ARRB2 complex occurred. An increase in the luminescent signal at a low speed was

dx.doi.org/10.1021/cb200360z | *ACS Chem. Biol.* 2012, 7, 901−910

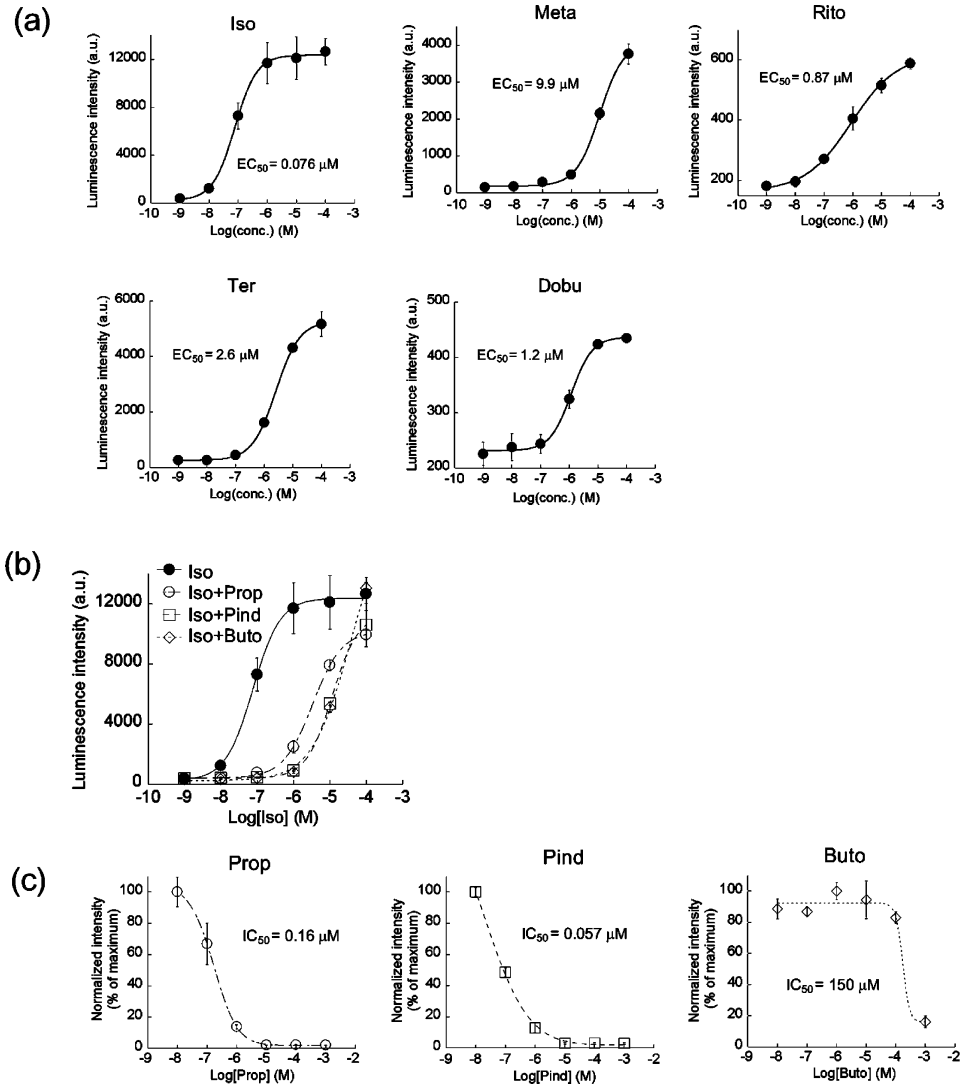

Figure 3. *In vitro* plate assays upon stimulation with ligands for ADRB2 using HEK293_FN-ARRB2_ADRB2-FC. (a) Dose−response curves for several agonists for ADRB2, such as Iso, metaproterenol (Meta), ritodrine (Rito), terbutaline (Ter), and dobutamine (Dobu), based on ADRB2−ARRB2 interaction. The cells were cultured on 96-well microtiter plates and stimulated for 10 min. The mean luminescence intensities were determined at each ligand concentration (n = 3). The EC_{50} values of the agonists were calculated. (b) Dose−response curves for Iso in the presence of competitive inhibitors, propranolol (Prop), pindolol (Pind), and butoxamine (Buto). Before stimulation with Iso, the cells were pretreated for 30 min with constant concentrations of the inhibitors: 1×10^{-7} M Prop, 1×10^{-7} M Pind, 1×10^{-4} M Buto (final). The mean luminescence intensities were determined at each ligand concentration (n = 3). (c) Inhibition assays for Iso in the presence of competitive inhibitors. After treatment with each concentration of antagonist, the cells were stimulated with 1×10^{-5} M Iso (final). The mean luminescence intensities were determined at each ligand concentration (n = 3).

triggered by stimulation of Meta, suggesting that the difference between Iso and Meta represent the duration of efficiency: Iso <1 h, and Meta 3−4 h. Regarding pretreatment with a competitive inhibitor, Prop, bioluminescence was not detected at all (Figure 4b). These results differed slightly from those of our previous studies,[23] in which the luminescence increased more slowly and the distribution of the luminescence was not changed. This may be true because the split luciferase probe based on Fluc can complement faster than that based on Eluc, which has been demonstrated previously using the same target proteins and assay protocol.[26] Therefore, this probe might provide more accurate information for live cell imaging.

Detection of Downstream Signaling. GPCR signaling varies depending on the cellular milieu. Therefore, multifunctional activities must be assessed in drug screening studies.[6] Accordingly, we tried to investigate the downstream signaling of ADRB2 by detection of second messengers. This report describes genetically encoded cAMP bioluminescent probe emitting green light: ElucN-PKA-Mcluc1.[14] Using an appropriate filter, the green signal emitted from Eluc is separable from whole bioluminescence from Fluc and Eluc (Supplementary Figure S4). To examine the generation of cAMP in HEK293_FN-ARRB2_ADRB2-FC, the cAMP probe was expressed transiently in the cells, and the bioluminescence was measured using a microplate reader with the filter through green light only (500 ± 7.5 nm). In the absence of cAMP probe, little luminescence was detected, indicating that the influence of the leakage from Fluc was limited (Figure 5a). In the presence of cAMP probe, luminescence was observed. It showed a dose−response sigmoidal curve against each concentration of Iso. Furthermore, we examined the calcium imaging of this cell line using a fluorescent calcium indicator,

dx.doi.org/10.1021/cb200360z | ACS Chem. Biol. 2012, 7, 901−910

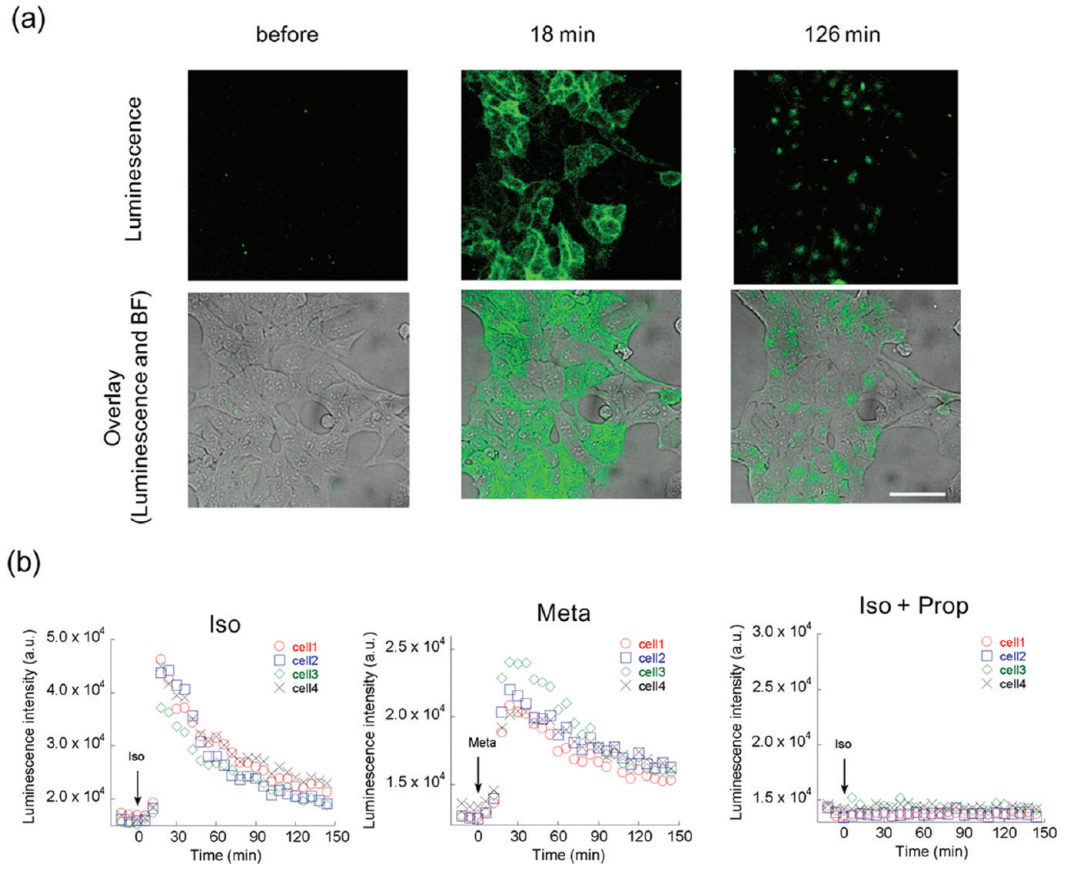

Figure 4. Live cell images of HEK293_FN-ARRB2_ADRB2-FC upon stimulation with agonists. (a) Real time bioluminescence images of ADRB2−ARRB2 interaction. The cells were stimulated with 1×10^{-6} M Iso (final). The injection time was defined at 0 min. Bioluminescence images were acquired every 6 min, of which interval bright field (BF) images were taken using an EM-CCD camera. The obtained bioluminescence (green) images were superimposed on the BF images. Scale bar: 20 μm. (b) Kinetics of bioluminescence upon stimulation with ligands such as Iso, Meta, and Prop.

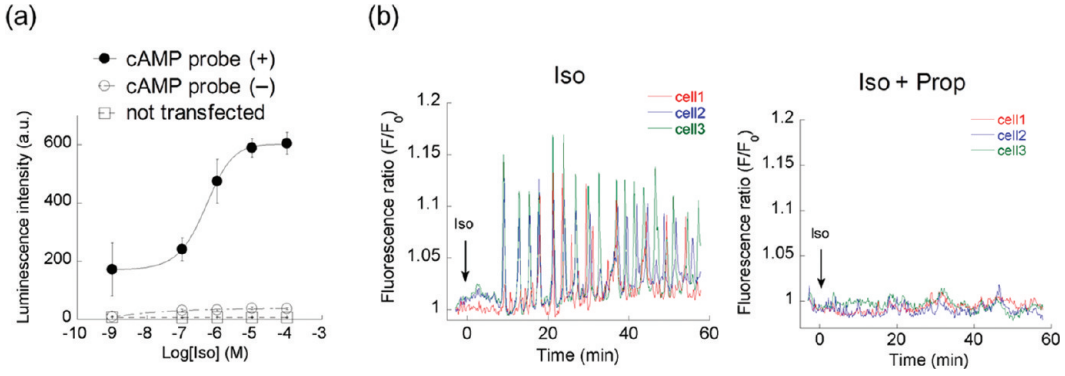

Figure 5. Detection of downstream signaling of HEK293_FN-ARRB2_ADRB2-FC upon stimulation with Iso. (a) Dose−response curve of cAMP against each concentration of Iso based on genetically encoded cAMP bioluminescence probe emitting green light. The cells were cultured on 96-well microtiter plates and were transiently transfected with the cAMP probe. After stimulation with Iso for 30 min, the bioluminescence was measured using a plate reader with the filter passed through only green light (500 ± 7.5 nm). The mean luminescence intensities were determined at each ligand concentration (n = 3). (b) Kinetics of influx of Ca^{2+} inside the cell on stimulation with Iso. The cells were cultured in a 35 mm dish and incubated for 1 h with the calcium indicator Fluo4. After washing, fluorescence was observed using upright fluorescence microscopy; 1×10^{-6} M Iso (final) was added to the dish as stimulation. For inhibition assays, 1×10^{-5} M Prop (final) was pretreated for 5 min.

Fluo4. As Figure 5b shows, intense and frequent calcium oscillation resulted from addition of Iso, but in the presence of Prop, the oscillation was inhibited (see Supplementary Movies S2 and S3). Consequently, this cell line is applicable not only for detection of the ADRB2−ARRB2 interaction but also for other functional assays such as generation of cAMP and influx of Ca^{2+}.

***In Vivo* Imaging of the ADRB2−ARRB2 Interaction.** In addition to the cell-based assays described above, it is important to evaluate the efficacy of potential chemicals for uses as drugs *in vivo* for screening. Herein, we examined *in vivo* systems of

dx.doi.org/10.1021/cb200360z | *ACS Chem. Biol.* 2012, 7, 901−910

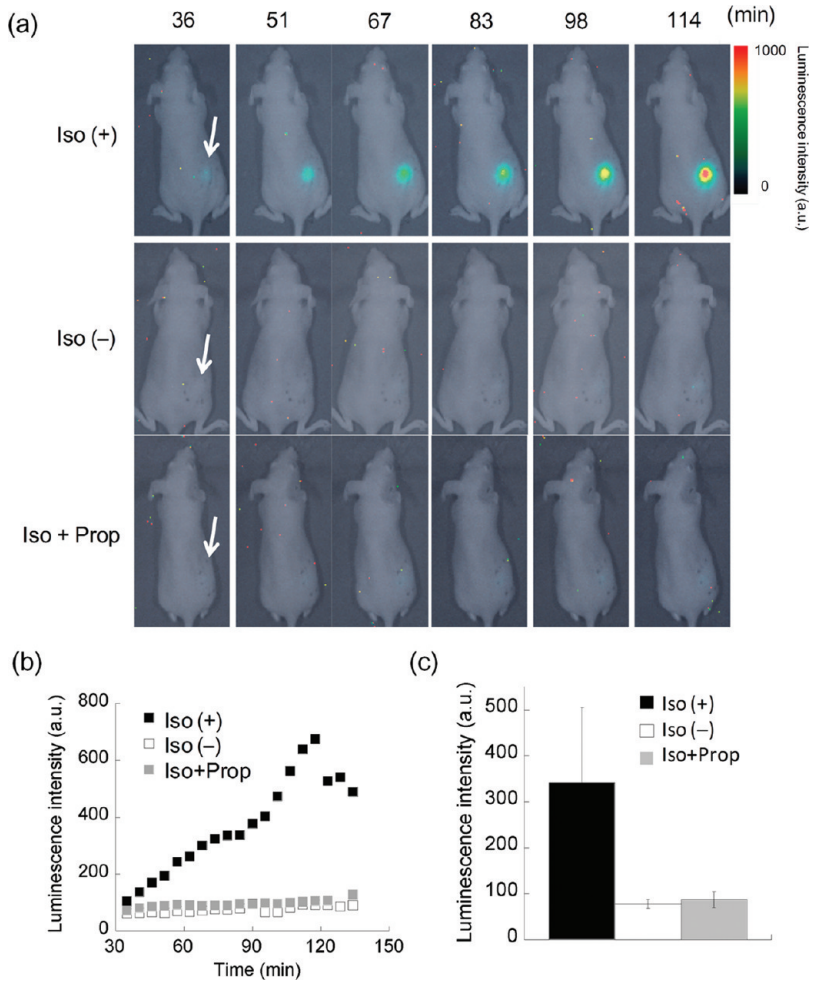

Figure 6. Bioluminescence *in vivo* imaging (BLI) of the ADRB2−ARRB2 interaction using mice implanted with HEK293_FN-ARRB2_ADRB2-FC cells. (a) BLI of the mice upon intraperitoneal (i.p.) injection of Iso. Cells were cultured in a 10 cm dish and harvested using a rubber scraper. The collected cells were suspended with PBS with D-luciferin (90 mg/kg body weight) and implanted under the skin of mice. Furthermore, the ligands were i.p. injected. The injection time was defined at 0 min. Thirty minutes after i.p. injection, BLI were taken every 5.5 min using a CCD camera under isoflurane anesthesia. The arrows indicate the location of cell implantation. (b) Kinetics of bioluminescence in the area of the cells. (c) Bioluminescence intensities at the time point of 120 min in the area of the cells. The luminescence intensities were averaged. They are represented along with the standard deviation (n = 3).

two kinds: subcutaneous cell implantation using HEK293_FN-ARRB2_ADRB2-FC and a HTV method, which enables us to introduce the plasmid DNA into organs of living animals, such as the liver, kidney, spleen, lung, and heart.[31,32] These two methods are easy and convenient, in contrast to infection of virus and creation of transgenic mice, because the two methods merely require the preparation of cells or plasmids containing a probe. For cell implantation, the collected cells were suspended in PBS including D-luciferin and implanted under the skin of a nude mouse's hind leg, in which dispersion or metabolism of D-luciferin was ignorable for a few hours (Supplementary Figure S5). Then, bioluminescence *in vivo* imaging (BLI) was conducted using a cooled CCD camera with or without Iso administered intraperitoneally (i.p.) (Figure 6). The luminescence from the back of the mouse increased gradually during 2 h, although no significant change was observed in the absence of Iso. For simultaneous i.p. injection of Iso and Prop, the increase in bioluminescence was inhibited completely, indicating that the ADRB2−ARRB2 interaction is detectable from the skin surface in live animals. Next, we examined BLI in liver, using mice treated with HTV. Saline solution containing the two plasmids of FN-ARRB2 and ADRB2-FC was prepared and injected at once into a tail vein. After 16−24 h of i.v. injection, BLI was obtained with or without Iso (Figure 7). The images show the luminescence signal from the liver after i.p. injection of Iso, but in the absence of Iso, little bioluminescence was observed. The luminescence upon stimulation with Iso was decreased gradually for 40 min. The decrease in the luminescence originated from the metabolism or consumption of D-luciferin, which was confirmed by a control experiment using full-length luciferase (Supplementary Figure S6). In the case of simultaneous i.p. injection of Iso and an inhibitor of Prop, the bioluminescence intensity was almost identical to that in the absence of Iso, indicating that the increased intensity upon stimulation with Iso represented the response of the ADRB2−ARRB2 interaction. In addition, bioluminescence intensities in the presence of Iso over 40 min were the same as those in the absence of Iso or in the presence of Prop. When we considered the rate of D-luciferin metabolism, the results indicated that the obtained bioluminescence intensities were almost independent of the metabolism of D-luciferin. In contrast, using split luciferase based on Eluc emitting shorter

dx.doi.org/10.1021/cb200360z | *ACS Chem. Biol.* 2012, 7, 901−910

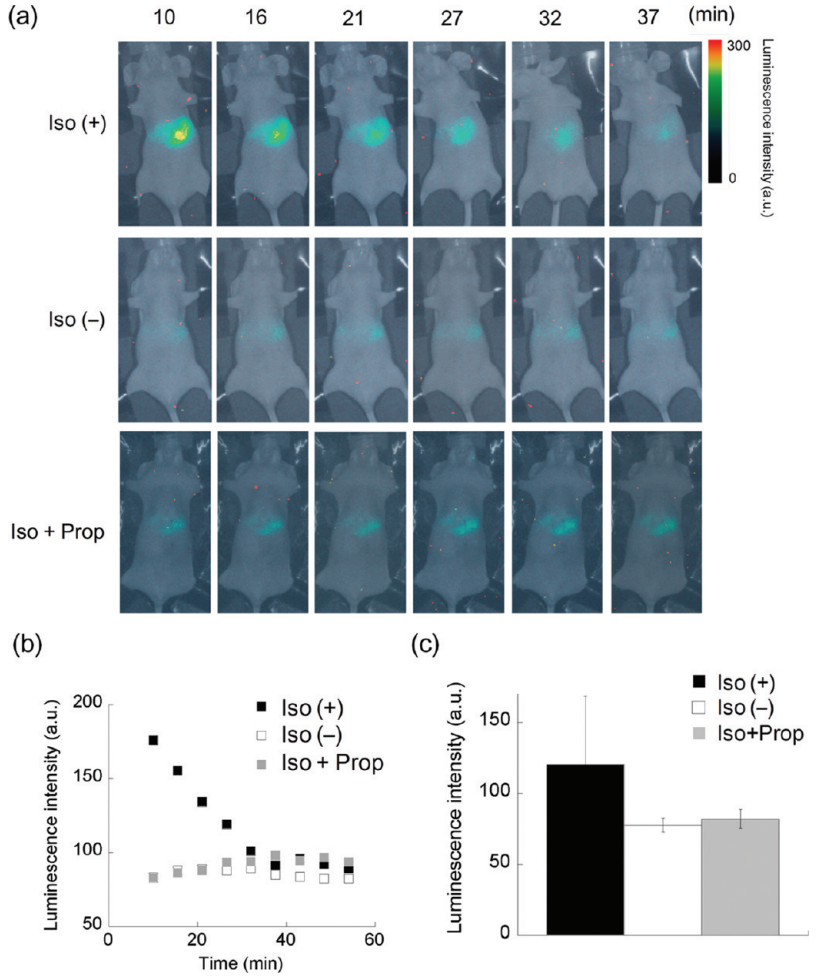

Figure 7. BLI of the ADRB2−ARRB2 interaction using mice treated with HTV. (a) BLI of the mice upon intraperitoneal (i.p.) injection of Iso. The mice were treated with HTV using FN-ARRB2 and ADRB2-FC 1 day before measurement. D-Luciferin (600 mg/kg body weight) and the ligands were i.p. injected; the injection time was defined at 0 min. After i.p. injection, BLI was taken every 5.5 min using a CCD camera under isoflurane anesthesia. (b) Kinetics of bioluminescence in the area of the cells. (c) Bioluminescence intensities at the time point of 10 min in the area of the cells. The luminescence intensities were averaged. They are represented along with the standard deviation (n = 3).

wavelength light, the signal in this system could not be visualized because of absorption of hemoglobin and light interference with tissues (data not shown). Therefore, we found it possible to take bioluminescence images *in vivo* from the liver merely by changing the luminescence wavelength. These results not only show accomplishment of visualization of ADRB2−ARRB2 interaction in the liver but also highlight the possibility of validating the efficiency of chemicals in the intact systems of available mice. In fact, the formerly used *in vivo* system, cell implantation, shows the phenomena in cultured cells. This *in vivo* system will be able to contribute to effective evaluation in pharmacokinetics and pharmacodynamics and expedite the development of new drugs for GPCRs.

Discussion. We demonstrated that the GPCR−β-arrestin interaction in mice liver was detectable using the split Fluc probe. It is well-known that the bioluminescence spectrum of Fluc depends on its surrounding environment such as pH condition, concentration of salts, and temperature. We then investigated the spectra of the split Fluc in *in vitro* assays and living cells and showed that the spectra were almost identical to that of full-length Fluc (Supplementary Figures S2 and S4). However, we could not analyze the spectrum in living mice because of a small number of photons. In previous reports, it has been shown that the absorbance of hemoglobin is drastically decreased over 600 nm.[24,25] We then estimated ratios of spectral area of different luciferases over 600 nm to the total area (Supplementary Figure S4). The percentage of bioluminescence from Eluc over 600 nm was only 7%, whereas that from Fluc remained 24%, indicating that absorbance of hemoglobin significantly influences the luminescence intensity from living tissue samples, and Fluc is more useful than Eluc for *in vivo* analysis. The other probes emitting red light, such as split CBRluc and red-shifted split Fluc, may be more suitable for *in vivo* imaging. However, these probes showed worse signal-to-noise ratios and lower luminescence intensities upon stimulation with Iso. Considering these results, we concluded that the split Fluc probe was most suitable for detecting the GPCR−β-arrestin interaction from deep tissues in living mice.

A difference of emission maxima between Eluc and Fluc is only 21 nm. Therefore, slight leakage from Fluc was observed within the region (used filter, 500 ± 7.5 nm) (Supplementary Figure S4a). We estimated the percentage of the leakage of Fluc over the total area and obtained the value of 0.3%. Because absolute value of bioluminescence intensity obtained from the ADRB2−ARRB2 interaction upon stimulation with Iso in *in vitro* plate assays was about 10,000, the value of the leakage

dx.doi.org/10.1021/cb200360z | *ACS Chem. Biol.* 2012, 7, 901−910

corresponded approximately to 30. In contrast, values of the background signals for the concentrations over 1×10^{-6} M Iso in Figure 5a were about 25, which were well consistent with the calculated background signal of Fluc. Also the value was only <5% compared to the signal obtained from ElucN-PKA-Mcluc1 upon stimulation with Iso through the filter. Taken together, we concluded that the filter enabled removal of most of the signal leaked from Fluc.

We demonstrated two *in vivo* detection methods of GPCR–β-arrestin interactions in this study: cell implantation and HTV methods. The administration procedures of D-luciferin between the two methods were different. In the case of cell implantation, D-luciferin was premixed to the cell solution. Therefore, the substrate was kept at the site of injection of cells, and the metabolism or consumption was not a serious problem over a few hours (Supplementary Figure S5). On the other hand, in order to deliver D-luciferin to mice livers, we administered the substrate intraperitoneally. In this case, D-luciferin is rapidly metabolized and consumed after injection (Supplementary Figure S6), which was consistent with a previous study.[33] It is important to note that the two methods provide different information: in cell implantation, the signal represents the distribution of chemical reagents at the site of injection of the cells because metabolism of D-luciferin less affected, whereas in the HTV method, the signal indicates the efficacy of chemical reagents in the endogenous system just at the time of i.p. injection of D-luciferin. The two methods can be discriminated for the purpose of the studies and provide different information of chemical reagents.

The *in vivo* detection of GPCR–β-arrestin interaction, especially using the HTV method, is a strong advantage for evaluation of the therapeutic reagents over previous ones. For *in vivo* imaging of GPCR–β-arrestin interactions, several methods have been developed to date; one existing method is the use of split β-gal probe to assess the association of GPCRs and β-arrestin.[20] However, the limitation of β-gal complementation for *in vivo* imaging is the necessity of caged luciferin, which has no emission light prior to hydrolysis by β-gal, for conversion of the enzymatic activity to bioluminescence signal. This two-step process increases the complexity of the assay procedure. Our present method used a one-step complementation system with Fluc fragments. A related technique is the imaging of CXCR4–β-arrestin interaction using Fluc complementation.[22] This showed BLI from the abdomen upon stimulation with ligands using mice implanted with the cells expressing the probe in good signal-to-noise ratios. However, the cell implantation system represents the condition inside the cultured cells. In contrast, the method using HTV has a great advantage. The plasmids encoding the probe can be introduced into the organs in living animals, and the expressed probe functions using the endogenous systems, which indicates that, using the present method, we can easily and noninvasively screen the efficacy of chemicals for the animals at the organs in *in vivo* testing. The site of the expression can be changed by the organ-specific promoters, although we used a CMV promoter in this study. This is a first demonstration that GPCR–β-arrestin interaction can be visualized directly in real time and noninvasively at the organ level in living animals.

Conclusion. We developed a method to detect ADRB2–ARRB2 interaction in *in vitro* plate assays, single living cell imaging, and *in vivo* imaging. Generating a cell line that stably expresses the split luciferase fragments emitting longer wavelength light, we demonstrated the applicability of the efficacy, EC_{50} and IC_{50} analysis to agonists and antagonists, respectively, using 96-well microtiter plates. This cell line was also applied to bioluminescence imaging in single living cells, indicating that the localization of the interaction and difference of kinetics between ligands can be studied. Furthermore, in two kinds of *in vivo* systems, cell implantation and HTV methods, the ADRB2–ARRB2 interaction was monitored using a cooled CCD camera, indicating that this split luciferase probe is applicable not only just under the skin but also in deeper tissues. It is noteworthy that we can visualize the ADRB2–ARRB2 interaction using the intact *in vivo* system of mice. This property engenders effective drug evaluation in pharmacodynamics and pharmacokinetics. The results presented above illustrate another advantage of the system: in different assay systems, we can perform screening and validation of potentially therapeutic compounds using the same detection format. Additionally, we examined the detection of second messengers, generation of cAMP, and influx of Ca^{2+} in the cell line expressing split luciferase probe, ensuring that it is applicable to multifunctional screenings. Obtained quick and robust signals will be applicable to *in vitro* HTS assay with an enormous chemical library, and hit compounds can be moved easily to the next assays, such as living biological samples. Consequently, using this method will bring great benefit to development of the new drugs for GPCRs.

METHODS

Materials and Construction of Mammalian Expression Vectors. See Supporting Information.

Cell Culture, Transfection, and Generation of Stable Expression Cell Lines. Human embryonic kidney (HEK293) cells were cultured in Dulbecco's modified eagle's medium (DMEM) (high glucose) supplemented with 10% fetal bovine serum (FBS), 100 unit/mL penicillin, and 100 μg/mL streptomycin at 37 °C in an atmosphere of 5% (v/v) CO_2. Transfection of plasmids into the cells was performed with reagents TransIT Transfection or Lipofectamine 2000. For establishment of the stable cell line, the transfected cells were screened with 2 mg/mL G418 or both 2 mg/mL G418 and 0.1 mg/mL Zeocin in the culture medium. For the culture of the stable cell line, the cells were incubated with 0.8 mg/mL G418 or both 0.8 mg/mL G418 and 0.04 mg/mL Zeocin in the culture medium.

Bioluminescence *in Vitro* Assays of the ADRB2–ARRB2 Interaction. In the transient transfection assays, HEK293 cells were incubated in 96-well microtiter plates and transfected with ARRB2 and ADRB2 fused with split luciferase fragments with 100 μL/well of a phenol red free DMEM supplemented with 10% FBS. After addition of 1×10^{-5} M Iso (final) or phosphate-buffered saline (PBS) to the medium, further incubation for 15 min at 37 °C was conducted. The luciferase activity was measured using a 96-well microplate reader (Tristar LB941; Berthold Technologies GmbH and Co. KG) with 50 μL/well of Bright-Glo. For the HEK293 cells that stably expressed FN-ARRB2 and ADRB2-FC, the cells were cultured with 100 μL/well of a phenol red free DMEM supplemented with 10% FBS, 100 unit/mL penicillin, and 100 μg/mL streptomycin and incubated at 37 °C in 5% CO_2. The cells were stimulated with different concentrations of agonists incubated for 10 min at 37 °C in 5% CO_2. For inhibition assays, the cells were pretreated with different concentrations of competitive inhibitors for 30 min at 37 °C in 5% CO_2. The luciferase activity was measured using 50 μL/well of Bright-Glo. The time for measuring each well was set at 2 s/well. All measurements were performed three or four times with different wells of plates. The averaged values were presented along with standard deviations.

Immunostaining. The stable expression cell line HEK293_FN-ARRB2_ADRB2-FC was cultured on a cover glass coated with poly L-lysine (PLL) at 37 °C in 5% CO_2 for 48 h. The cells were stained with Hoechst 33342 (1.0 μg/mL) for 30 min and washed with PBS. Then

dx.doi.org/10.1021/cb200360z | ACS Chem. Biol. 2012, 7, 901–910

the cells were fixed with 4% paraformaldehyde in the culture dish at 37 °C for 30 min and washed with PBS. The cells were permeabilized with 0.2% TritonX-100 in PBS for 5 min and subsequently washed three times with PBS. The cells were blocked by 0.2% fish skin gelatin (FSG) in PBS for 18 h at 4 °C. For the staining of ADRB2, the buffer was exchanged to PBS (0.2% FSG) containing a 1/1000 dilution of mouse anti-V5 antibody and incubated for 2 h at RT with gentle shaking. After washing the cells with PBS, the cells were filled with PBS (0.2% FSG) containing a 1/2000 dilution of a donkey anti-mouse IgG labeled with AlexaFluoro 488 and incubated for 1 h at RT. For ARRB2 staining, a 1/1000 dilution of mouse Myc antibody and AlexaFluoro 488 donkey anti-mouse IgG were used, respectively, as first and second antibodies. Cells were washed with PBS (0.2% FSG) and fixed on a cover glass with Mowiol. The cells labeled with fluorescent molecules were observed under a confocal microscope (FV-1000; Olympus Corp.).

Live Cell Imaging. The stable cell line HEK293_FN-ARRB2_ADRB2-FC was incubated on 35 mm culture dishes coated with PLL in DMEM with 10% FBS for 36−48 h at 37 °C in 5% CO_2. Before taking bioluminescence images, culture medium was exchanged to Hank's balanced buffered saline (HBSS) containing 10% FBS and 4 mM D-luciferin, and incubated at 37 °C for 15 min. Bioluminescence images of live cells were taken using an upright bioluminescence microscope (BX61; Olympus Corp.), which was used with a 40× dipping objective. Eighteen minutes after measurements were started, 1×10^{-6} M Iso or 1×10^{-5} M Meta (final) was added to the dishes. For inhibition assays, the dishes were pretreated with 1×10^{-5} M Prop (final) 30 min before taking images. For bioluminescence imaging, we used only an emission long-pass filter. Digital images were acquired using a cooled (set at −80 °C) electron multiplying charge-coupled device (EM-CCD) camera (ImagEM-1K; Hamamatsu Photonics K.K.). Stray light was cut off by turning off the electric system and covering it tightly with foil. The exposure times were 5 min for bioluminescence images and 100 ms for DIC images. Bioluminescence images were acquired every 6 min. The obtained images were analyzed using imaging software (Meta Morph; Universal Imaging Corp.).

***In Vivo* Imaging.** For cell implantation, HEK293_FN-ARRB2_ADRB2-FC cells were cultured in 10-cm dishes with DMEM supplemented with 10% FBS and were incubated for 48 h at 37 °C in 5% CO_2. The cells were harvested with rubber scrapers and suspended in PBS containing D-luciferin (90 mg/kg of body weight). Then an aliquot of 5×10^6 cells was implanted on the back of BALB/c-nude mouse (female, 5−8 weeks old, 17−22 g body weight). After implantation of the cells, 150 μL of 20 mM Iso was injected intraperitoneally (i.p.). Thirty minutes after injection of Iso, the mouse was imaged with a cooled CCD camera (Versarray 1300B; Princeton Instruments Inc.) under isoflurane anesthesia. In the case of inhibition assays, 150 μL of 2 mM Prop was injected i.p. simultaneously with Iso. The exposure time was 5 min. Images were taken every 5.5 min. Image processing was performed using imaging software (SlideBook 4.1; Intelligent Imaging Innovation Inc.).

For the HTV method, 20 μg of FN-ARRB2 and ADRB2-FC, respectively, was dissolved in saline of about one-tenth of the body weight of mice. The solution was injected at once through a tail vein. After 18−24 h, 150 μL of 2 mM Iso and D-luciferin (600 mg/kg of body weight) were injected i.p. In the case of inhibition assays, 150 μL of 20 mM Prop was injected i.p. simultaneously with Iso. BLI was taken with a cooled CCD camera under isoflurane anesthesia. The exposure time was 5 min. Images were taken every 5.5 min. Image processing was performed using imaging software (SlideBook 4.1).

cAMP Assay. The stable cell line was cultured with 100 μL/well of DMEM supplemented with 10% FBS, 100 unit/mL penicillin, and 100 μg/mL streptomycin and incubated at 37 °C in 5% CO_2. Transfection of the cDNA of the cAMP probe, ElucN-PKA-Mcluc1,[14] was performed with Lipofectamine 2000. The cells were stimulated with different concentrations of Iso incubated for 30 min at 37 °C in 5% CO_2. The luciferase activity was measured using a microplate reader with a filter passing only green light (500 nm ± 7.5 nm) with 50 μL/well Bright-Glo. The time for measurement was 2 s/well. All measurements were performed three times with different wells of plates. The values were averaged and presented along with standard deviations.

Calcium Imaging. The cells were cultured on 35 mm culture dishes coated with PLL in DMEM supplemented with 10% FBS, 100 unit/mL penicillin, and 100 μg/mL streptomycin for 36−48 h at 37 °C in 5% CO_2. Before taking the fluorescence images, the culture medium was exchanged to a phenol red free DMEM containing 25 mM HEPES and 2 μM Fluo4, with subsequent incubation at 37 °C for 60 min. Fluorescence images of live cells were taken with an upright fluorescence microscope (BX61; Olympus Corp.), which was used with a 40× dipping objective. At 3 min after starting measurements, 1×10^{-6} M Iso (final) was added to the dishes. For inhibition assays, the dishes were pretreated with 1×10^{-5} M Prop (final) for 5 min before taking images. For fluorescence imaging, we used only an emission band-pass filter (531 ± 16 nm). Digital images were acquired using a cooled (set at −80 °C) EM-CCD camera. Stray light was cut off by turning off the electric system and covering it tightly with foil. The exposure times were 200 ms for fluorescence images and 100 ms for DIC images. The fluorescence images were acquired every 10 s. The obtained images were analyzed using imaging software (Meta Morph).

■ ASSOCIATED CONTENT

Ⓢ Supporting Information

This material is available free of charge via the Internet at http://pubs.acs.org.

■ AUTHOR INFORMATION

Corresponding Author

*E-mail: ozawa@chem.s.u-tokyo.ac.jp.

Notes

The authors declare no competing financial interest.

■ ACKNOWLEDGMENTS

This work was supported by the Japan Society for the Promotion of Science (JSPS), New Energy Industrial Technology Development Organization (NEDO), and in part by the Global COE Program and grants (S0801035), MEXT, Japan.

■ REFERENCES

(1) Musnier, A., Blanchot, B., Reiter, E., and Crepieux, P. (2010) GPCR signalling to the translation machinery. *Cell. Signal. 22*, 707−716.

(2) Dorsam, R. T., and Gutkind, J. S. (2007) G-protein-coupled receptors and cancer. *Nat. Rev. Cancer 7*, 79−94.

(3) Conn, P. J., Christopoulos, A., and Lindsley, C. W. (2009) Allosteric modulators of GPCRs: a novel approach for the treatment of CNS disorders. *Nat. Rev. Drug Discovery 8*, 41−54.

(4) Alkhalfioui, F., Magnin, T., and Wagner, R. (2009) From purified GPCRs to drug discovery: the promise of protein-based methodologies. *Curr. Opin. Pharmacol. 9*, 629−635.

(5) Kenakin, T. P. (2009) Cellular assays as portals to seven-transmembrane receptor-based drug discovery. *Nat. Rev. Drug Discovery 8*, 617−626.

(6) Allen, J. A., and Roth, B. L. (2011) Strategies to discover unexpected targets for drugs active at G protein-coupled receptors. *Annu. Rev. Pharmacol. Toxicol. 51*, 117−144.

(7) Pert, C. B., and Snyder, S. H. (1973) Opiate receptor: demonstration in nervous tissue. *Science 179*, 1011−1014.

(8) Pert, C. B., Pasterna., G., and Snyder, S. H. (1973) Opiate agonists and antagonist discriminated by receptor binding in brain. *Science 182*, 1359−1361.

(9) Haugland, R. P. (2005) *Handbook of Fluorescent Probes and Research Products*, 10th ed., Molecular Probes, Inc., Eugene, OR.

(10) Mank, M., and Griesbeck, O. (2008) Genetically encoded calcium indicators. *Chem. Rev. 108*, 1550−1564.

(11) Paredes, R. M., Etzler, J. C., Watts, L. T., Zheng, W., and Lechleiter, J. D. (2008) Chemical calcium indicators. *Methods 46*, 143−151.
(12) Willoughby, D., and Cooper, D. M. F. (2008) Live-cell imaging of cAMP dynamics. *Nat. Methods 5*, 29−36.
(13) Fan, F., Binkowski, B. F., Butler, B. L., Stecha, P. F., Lewils, M. K., and Wood, K. V. (2008) Novel genetically encoded biosensors using firefly luciferase. *ACS Chem. Biol. 3*, 346−351.
(14) Takeuchi, M., Nagaoka, Y., Yamada, T., Takakura, H., and Ozawa, T. (2010) Ratiometric bioluminescence indicators for monitoring cyclic adenosine 3 ′,5 ′-monophosphate in live cells based on luciferase-fragment complementation. *Anal. Chem. 82*, 9306−9313.
(15) Milligan, G. (2004) Applications of bioluminescence and fluorescence resonance energy transfer to drug discovery at G protein-coupled receptors. *Eur. J. Pharm. Sci. 21*, 397−405.
(16) Hamdan, F. F., Audet, M., Garneau, P., Pelletier, J., and Bouvier, M. (2005) High-throughput screening of G protein-coupled receptor antagonists using a bioluminescence resonance energy transfer 1-based β-arrestin2 recruitment assay. *J. Biomol. Screen. 10*, 463−475.
(17) Masri, B., Salahpour, A., Didriksen, M., Ghisi, V., Beaulieu, J. M., Gainetdinov, R. R., and Caron, M. G. (2008) Antagonism of dopamine D2 receptor/β-arrestin 2 interaction is a common property of clinically effective antipsychotics. *Proc. Natl. Acad. Sci. U.S.A. 105*, 13656−13661.
(18) Barnea, G., Strapps, W., Herrada, G., Berman, Y., Ong, J., Kloss, B., Axel, R., and Lee, K. J. (2008) The genetic design of signaling cascades to record receptor activation. *Proc. Natl. Acad. Sci. U.S.A. 105*, 64−69.
(19) Huang, X. P., Setola, V., Yadav, P. N., Allen, J. A., Rogan, S. C., Hanson, B. J., Revankar, C., Robers, M., Doucette, C., and Roth, B. L. (2009) Parallel functional activity profiling reveals valvulopathogens are potent 5-hydroxytryptamine$_{2B}$ receptor agonists: implications for drug safety assessment. *Mol. Pharmacol. 76*, 710−722.
(20) von Degenfeld, G., Wehrman, T. S., Hammer, M. M., and Blau, H. M. (2007) A universal technology for monitoring G-protein-coupled receptor activation *in vitro* and noninvasively in live animals. *FASEB J. 21*, 3819−3826.
(21) Hammer, M. M., Wehrman, T. S., and Blau, H. M. (2007) A novel enzyme complementation-based assay for monitoring G-protein-coupled receptor internalization. *FASEB J. 21*, 3827−3834.
(22) Luker, K. E., Gupta, M., and Luker, G. D. (2008) Imaging CXCR4 signaling with firefly luciferase complementation. *Anal. Chem. 80*, 5565−5573.
(23) Misawa, N., Kafi, A. K. M., Hattori, M., Miura, K., Masuda, K., and Ozawa, T. (2010) Rapid and high-sensitivity cell-based assays of protein-protein interactions using split click beetle luciferase complementation: an approach to the study of G-protein-coupled receptors. *Anal. Chem. 82*, 2552−2560.
(24) Weissleder, R. (2001) A clearer vision for *in vivo* imaging. *Nat. Biotechnol. 19*, 316−317.
(25) Weissleder, R., and Ntziachristos, V. (2003) Shedding light onto live molecular targets. *Nat. Med. 9*, 123−128.
(26) Hida, N., Awais, M., Takeuchi, M., Ueno, N., Tashiro, M., Takagi, C., Singh, T., Hayashi, M., Ohmiya, Y., and Ozawa, T. (2009) High-sensitivity real-time imaging of dual protein-protein interactions in living subjects using multicolor luciferases. *PLoS ONE 4*, e5868.
(27) MacGregor, D. A., Prielipp, R. C., Butterworth, J. F., James, R. L., and Royster, R. L. (1996) Relative efficacy and potency of β-adrenoceptor agonists for generating cAMP in human lymphocytes. *Chest 109*, 194−200.
(28) Cunliffe, J. M., Sunahara, R. K., and Kennedy, R. T. (2007) Detection of G protein coupled receptor mediated adenylyl cyclase activity by capillary electrophoresis using fluorescently labeled ATP. *Anal. Chem. 79*, 7534−7539.
(29) Drake, M. T., Violin, J. D., Whalen, E. J., Wisler, J. W., Shenoy, S. K., and Lefkowitz, R. J. (2008) β-Arrestin-biased agonism at the β_2-adrenergic receptor. *J. Biol. Chem. 283*, 5669−5676.
(30) Insel, P. A., Mahan, L. C., Motulsky, H. J., Stoolman, L. M., and Koachman, A. M. (1983) Time-dependent decreases in binding-affinity of agonists for β-adrenergic receptors of intact S49 lymphoma-cells. *J. Biol. Chem. 258*, 13597−13605.
(31) Liu, F., Song, Y. K., and Liu, D. (1999) Hydrodynamics-based transfection in animals by systemic administration of plasmid DNA. *Gene Ther. 6*, 1258−1266.
(32) Sebestyen, M. G., Budker, V. G., Budker, T., Subbotin, V. M., Zhang, G. F., Monahan, S. D., Lewis, D. L., Wong, S. C., Hagstrom, J. E., and Wolff, J. A. (2006) Mechanism of plasmid delivery by hydrodynamic tail vein injection. I. Hepatocyte uptake of various molecules. *J. Gene. Med. 8*, 852−873.
(33) Wehrman, T. S., von Degenfeld, G., Krutzik, P., Nolan, G. P., and Blau, H. M. (2006) Luminescent imaging of β-galactosidase activity in living subjects using sequential reporter-enzyme luminescence. *Nat. Methods 3*, 295−301.